Archives of Oral Biology 61 (2016) 149–155

Contents lists available at ScienceDirect

Archives of Oral Biology

journal homepage: www.elsevier.com/locate/aob

The membrane-associated MUC1 improves adhesion of salivary MUC5B on buccal cells. Application to development of an in vitro cellular model of oral epithelium

Sarah Ployon[a,b,c], Christine Belloir[a,b,c], Aline Bonnotte[d], Jeannine Lherminier[e], Francis Canon[a,b,c], Martine Morzel[a,b,c,*]

[a] CNRS, UMR 6265 Centre des Sciences du GoÛt et de l'Alimentation, F-21000 Dijon, France
[b] INRA, UMR1324 Centre des Sciences du GoÛt et de l'Alimentation, F-21000 Dijon, France
[c] Université de Bourgogne, UMR Centre des Sciences du GoÛt et de l'Alimentation, F-21000 Dijon, France
[d] Université de Bourgogne, UMR 1347 Agroécologie, Plateforme DImaCell, Centre de Microscopie INRA/Université de Bourgogne, F-21000 Dijon, France
[e] INRA, UMR1347 Agroécologie, ERL CNRS 6300, Plateforme DImaCell, Centre de Microscopie INRA/Université de Bourgogne, F-21000 Dijon, France

ARTICLE INFO

Article history:
Received 20 August 2015
Received in revised form 2 November 2015
Accepted 3 November 2015

Keywords:
Oral mucosa
Mucosal pellicle
TR146 cells
Mucins
Immunocytochemistry
Scanning electron microscopy

ABSTRACT

Objectives: The mucosal pellicle is a thin layer of salivary proteins, mostly MUC5B mucins, anchored to epithelial oral cells. This pellicle is involved in protection of oral mucosae against abrasion, pathogenic microorganisms or chemical xenobiotics. The present study aimed at studying the involvement of MUC1 in mucosal pellicle formation and more specifically in salivary MUC5B binding using a cell-based model of oral epithelium.
Design: MUC1 mRNAs were not detected in TR146 cells, and therefore a stable cell line named TR146/MUC1 expressing this protein was developed by transfection. TR146 and TR146/MUC1 were incubated with human saliva in order to evaluate retention of MUC5B by epithelial cells.
Results: The cell surface of both TR146 and TR146/MUC1 was typical of a squamous non-keratinized epithelium, with the presence of numerous microplicae. After incubation for 2 h with saliva diluted in culture medium (1:1) and two washes with PBS, saliva deposits on cells appeared as a loose filamentous thin network. MUC5B fluorescent immunostaining evidenced a heterogeneous lining of confluent cell cultures by this salivary mucin but with higher fluorescence on TR146/MUC1 cells. Semi-quantification of MUC5B bound to cells confirmed a better retention by TR146/MUC1, evaluated by Dot Blot (+34.1%, $p < 0.05$) or by immunocytochemistry (+44%, $p < 0.001$).
Conclusion: The membrane-bound mucin MUC1 is a factor enhancing the formation of the mucosal pellicle by increasing the binding of salivary MUC5B to oral epithelial cells. An in vitro model suitable to study specifically the function and properties of the mucosal pellicle is proposed.

1. Introduction

The oral cavity is lined by a thin layer of salivary proteins anchored onto mucosae (Bradway, Bergey, Jones, & Levine, 1989) and teeth (Hay, 1967), termed the mucosal and dental pellicles respectively. The mucosal pellicle is the inner structure of the protective mucus layer on mucosae, the upper structure being a mobile layer of saliva (Pramanik, Osailan, Challacombe, Urquhart, & Proctor, 2010). Salivary pellicles are known to have an essential role in oral health (Tabak, Levine, Mandel, & Ellison, 1982). For example, the dental pellicle ensures lubrication and buffering of dental surface (Hannig & Joiner, 2006). Regarding more specifically the mucosal pellicle, by similarity with the dental pellicle, it could contribute to moisture retention, lubrication or protection against microbial colonization (Bradway et al., 1989). It could also play a role in sensory perception of astringency (Nayak & Carpenter, 2008). Finally, similarly to intestinal mucus which is a gel barrier to drug delivery (Boegh & Nielsen, 2015), it is likely that the salivary mucus modulates diffusion properties of drugs and other chemical compounds through the oral mucosa (Teubl et al., 2013). Based on these functions of the mucosal pellicle, it appears necessary to include this biological structure to in vitro models of oral mucosa.

* Corresponding author at: INRA-CSGA, 17 rue Sully, 21000 Dijon, France. Fax: +33 380 69 32 27.
E-mail address: martine.morzel@dijon.inra.fr (M. Morzel).

http://dx.doi.org/10.1016/j.archoralbio.2015.11.002
0003-9969/

The mucosal pellicle contains salivary proteins such as amylase, IgA, cystatins (Bradway et al., 1989), carbonic anhydrase IV, secretory component or mucins (Gibbins, Yakubov, Proctor, Wilson, & Carpenter, 2014). Among these salivary proteins, MUC5B has been identified as a major component of *in vivo*(Gibbins, Proctor, Yakubov, Wilson, & Carpenter, 2014) and *in vitro*(Cardenas, Elofsson, & Lindh, 2007) mucosal pellicles. Detecting MUC5B on cells sampled from human buccal surfaces confirmed its attachment to epithelial cells (Morzel, Tai, Brignot, & Lherminier, 2014).

The mechanisms of pellicle formation are not fully understood. Hydrophobic effects between the cell surface and salivary proteins have been suggested to be a prominent factor in pellicle formation (Gibbins, Yakubov et al., 2014). Surface wettability has also been reported to be involved in the structural organization of pellicle components (Aroonsang, Sotres, El-Schich, Arnebrant, & Lindh, 2014). From a biochemical point of view, cross-linking between salivary components by transglutaminase was demonstrated (Bradway et al., 1992; Gibbins, Yakubov et al., 2014). The involvement of the membrane-bound mucins MUC1 in MUC5B adhesion to cells through direct binding between the two mucins has also been suggested (Gibbins, Yakubov et al., 2014; Offner & Troxler, 2000). A recent study further supported the hypothesis of a role of membrane-bound mucins, by demonstrating that MUC5B could bind to HT29 intestinal cells only when they were induced to secrete the membrane-bound mucins MUC5AC(Gibbins, Proctor, Yakubov, Wilson, & Carpenter, 2015).

MUC1 is a polymorphic membrane-associated glycoprotein (Hanisch & Muller, 2000), expressed in most healthy epithelial tissues. In relation to tissues of the human oral cavity, MUC1 mRNAs were found in salivary glands (Sengupta et al., 2001) but also in epithelial oral cells (Chang, Chang, Kim, Lee, & Kho, 2011). Recently, the protein MUC1 was detected in the superficial part of oral epithelium (Kullaa, Asikainen, Herrala, Ukkonen, & Mikkonen, 2014). Decrease of MUC1 levels in epithelial cells of elderly has been associated to lower mucosal defences in the oral cavity (Chang et al., 2011), supporting its implication in the formation of the mucosal pellicle.

The aim of the present study was to investigate the role of MUC1 in the binding of MUC5B to oral mucosae. We opted for a cell-based model using TR146 cells, which have been shown to be suitable for establishing a model of oral epithelium (Jacobsen, Van Deurs, Pedersen, & Rassing, 1995). TR146 cells were stably transfected in order to over-express MUC1, and adhesion of human salivary MUC5B on either transfected or native cell lines was compared. The resulting models, constituted of epithelial cells lined by a salivary pellicle, were characterized by microscopic approaches

2. Materials and methods

2.1. Saliva collection

The study was performed following the guidelines of the declaration of Helsinki. Written informed consent was obtained from the participants. Saliva was obtained from fifteen volunteers who declared to be in good oral health. Subjects were instructed to refrain from smoking, eating or drinking for at least two hours before saliva collection. Subjects donated saliva for approximately 1 h by spitting out saliva accumulating spontaneously in their mouth into plastic vessels. All samples were pooled and centrifuged at 14 000 g for 20 min at 4 °C. The resulting pool of clarified saliva was aliquoted and immediately frozen at – 80 °C.

2.2. Cell culture

TR146 epithelial cells, derived from a human buccal squamous cell carcinoma (Rupniak et al., 1985), were obtained from the European Collection of Cell Cultures (ECACC, Salisbury, Wiltshire, UK). TR146 cells were routinely grown in DMEM/F12—GlutaMAX medium from Gibco® (1:1, v:v), supplemented with 10% fetal bovine serum (FBS) and 100 units/ml penicillin, 100 μg/ml streptomycin in T75 flasks (all obtained from Life Technologies). Cells were subcultured at 7 days intervals and medium was changed every 2 days. Cells were incubated at 37 °C in a humidified atmosphere containing 7.5% CO_2. Cells were seeded at a density of 4×10^4 cells/cm^2 in 96-well plates for viability assay, in 12-well culture plates for semi-quantification of MUC5B by dot blot, in 8-well culture slides coated with Cell-Tak™ (Corning) for MUC5B and MUC1 immunostaining or on 10 mm diameter glass slips coated with Cell-Tak™ for Scanning Electron Microscopy (SEM) and confocal microscopy. In these conditions, confluence was reached in 48 h and cells formed a multi-layer culture after five days. Cells were grown for five days before depositing clarified saliva at the culture surface.

2.3. Exposure of cells to human saliva: viability assay and formation of a salivary pellicle

At confluence, cells were incubated for 24 h with clarified saliva diluted in growth medium (1:1, v:v). DMSO 50% was used as a positive control of cytotoxic effect. Cytotoxic effect of saliva was assessed using the Neutral Red assay using a fluorimetric method (Rat, Korwinzmijowska, Warnet, & Adolphe, 1994). Briefly, cells were incubated for 3 h at 37 °C with 200 μl of medium containing neutral red at 50 μg/ml, washed twice with PBS that was removed, and then incubated at room temperature for 1 h in neutral red eluent (ethanol:H_2O:acetic acid, 50:49:1) with gentle agitation. Reading of fluorescence was performed with Victor^{3}V microplate reader (PerkinElmer) with excitation and emission wavelengths fixed at 544 nm and 595 nm, respectively. 80% of viability was considered as an indicator of non-cytotoxicity. Assays were performed in triplicates.

A salivary pellicle was deposited onto cells by incubating cell subcultures for 2 h with clarified saliva diluted into growth medium (1:1). After incubation, samples were washed twice with PBS in order to eliminate the non-adsorbed saliva.

2.4. Measurement of the cell multi-layer thickness

Five-day subcultures were stained using LIVE/DEAD® BacLight™ (LifeTechnologies), which stains live cells with Syto 9 and dead cells with propidium iodide. Confocal microscopy was used in order to observe throughout the culture. Pictures were taken from the glass surface to the upper cells' surface with 160 nm steps imaging and were merged in order to obtain an overlay projection, which allowed evaluating the cell model thickness.

2.5. Cell transfection

The vector (pCMV6) carrying the gene of MUC1 variant 2 from OriGene (OriGene Technologies, ref. SC302125) was used. The protein encoded by the gene matches with the isoform Y of the human MUC1 (Uniprot identifier P15941-7). The plasmid was amplified by subcloning in DH5α *Escherichia coli* (Life Technologies) and purified using PureYield™ Plasmid Miniprep System (Promega). Cells were transfected when 80% confluence was reached. FuGENE®-HD (Promega) was used as transfection reagent at a FuGENE®-HD:DNA ratio of 3.0:1 following the manufacturer's instructions. After 48 h, cells were subjected to drug selection in 0.2 mg/ml geneticin (G418 sulfate, LifeTechnologies) for 2–3 weeks. Surviving cell colonies were then picked up and subcloned using cloning rings. Twenty-four clones were expanded stepwise in 96, 24, 6-well plates and screened for gene expression of MUC1

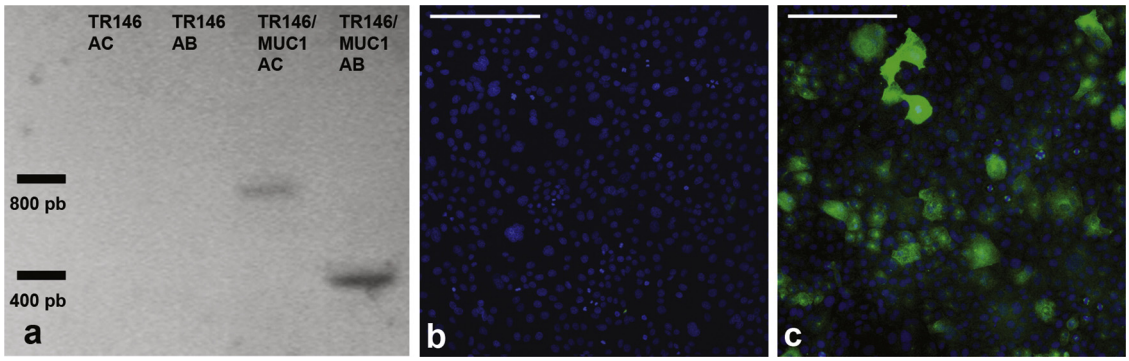

Fig. 1. Over-expression of MUC1 in TR146/MUC1 cells evidenced by (a) RT-PCR in native TR146 cells and transfected TR146/MUC1 cells, (b) and (c) immunostaining of MUC1 on TR146 and TR146/MUC1 transfected cells, respectively. Cell nuclei are stained in blue by DAPI. Scale bars 100 μm. (For interpretation of the references to color in this figure legend, the reader is referred to the web version of this article.)

by RT-PCR. The best stable cell line named TR146/MUC1 was obtained after 55 days of selection and growth.

2.6. Expression of MUC1 by RT-PCR

For preparation of cDNA from the cells, total RNA was extracted from TR146 and TR146/MUC1 confluent cells using RNAeasy Plus Mini Kit (QIAGEN) and quantified using a NanoDrop ND-1000 spectrophotometer (Thermo Scientific). Reverse transcription was performed using Biorad iScript™ cDNA Synthesis Kit on 450 ng of total RNA in a final volume of 10 μl. PCR was performed using Taq PCR Master Mix Kit (QIAGEN) with 2.5 μl of template DNA and 0.2 μM primers in a total reaction volume of 25 μl. The following cycling parameters were applied: 94 °C for 3 min and 30 cycles of amplification (94 °C for 50 s; 60 °C for 50 s and 72 °C for 2 min). Gene specific primers were designed according to standard recommendations with primer design software (Primer-Blast and Vector NTI® software). Two primers pairs were ordered at Eurogentec. A first pair (AB, 5′TGCTTACAGCTACCACAGCC3′ and 5′CCAGACTGGGCAGAGAAAGG3′) was designed in order to hybrid with all MUC1 mRNA forms (cDNA sequence of 436 pb). A second pair (AC, 5′TGCTTACAGCTACCACAGCC3′ and 5′ATTAGGACAAGGCTGGTGGG3′) was designed in order to target specifically insertion sequence MUC1 of 795 bp length specific for *pCMV6-MUC1* construction. Amplified products were resolved by agarose gel electrophoresis (0.8%) at 100 V for 20 min. Gel was stained with ethidium bromide and viewed under UV transilluminator Geldoc 2000 imaging system (Bio-Rad).

2.7. Fluorescence immunostaining of MUC1 and MUC5B

Immunostaining of MUC1 was performed on TR146 and TR146/MUC1 cells without a salivary pellicle. Immunostaining of MUC5B was performed on native or transfected cells with or without a salivary pellicle.

Samples on glass slides were fixed by immersion in cold methanol for 10 min. Non-specific binding was prevented using 0.3% fat-free milk and 5% non-immune goat serum in PBS for

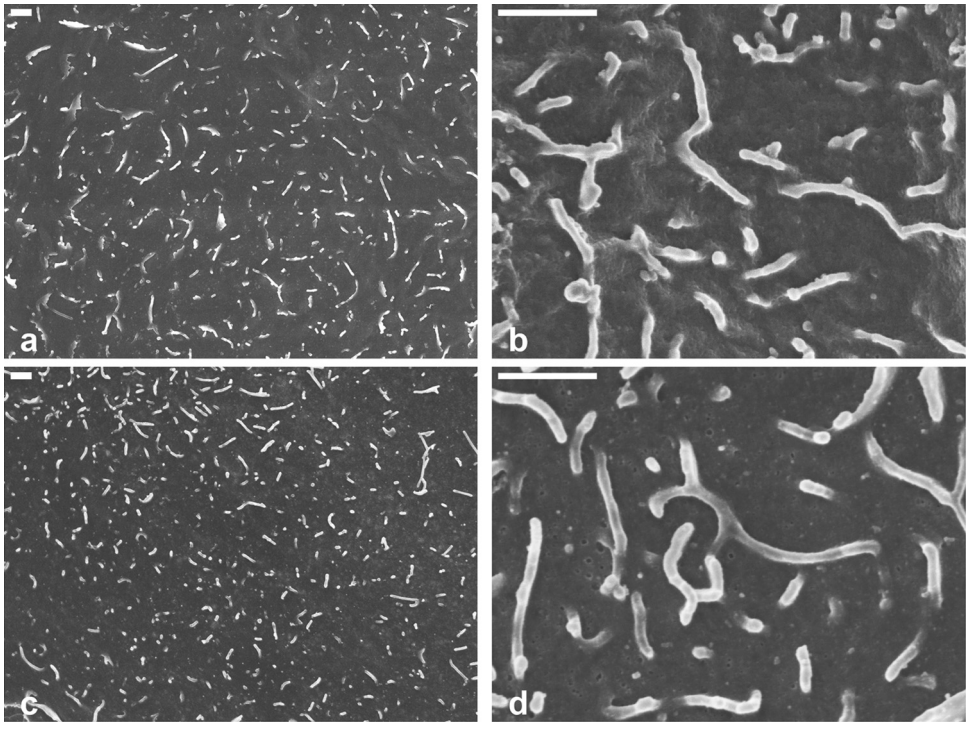

Fig. 2. TR146 (a and b) and TR146/MUC1 (c and d) cells observed by SEM. Scale bars 1 μm.

15 min. For MUC1 immunostaining, a mouse monoclonal anti-MUC1 antibody clone 4A5 (OriGene Technologies) was used (1:200 in PBS, 1 h). For MUC5B immunostaining, a mouse monoclonal anti-MUC5B antibody F2 (kind gift from Prof. Veerman, Free University of Amsterdam) was used (1:25 in PBS, 1.5 h). Negative controls were obtained by omitting primary antibodies in the incubation medium. Alexa 488 Goat anti-mouse IgG (Invitrogen) was used as the secondary antibody (1:400 in PBS, 1 h). The samples were mounted into Prolong Gold antifade reagent with DAPI (Invitrogen). Fluorescence was observed with a Nikon Eclipse E600 microscope (Nikon Instruments) equipped with UV-2A (excitation 330–380 nm, emission 400 nm) and B-2A (excitation 450–490 nm, emission 505 nm) filters. Images were acquired using a Nikon Dxm1200C camera. The Nikon NIS-Br software was used for data acquisition. MUC5B were semi-quantified using ImageJ software on 5 images of either TR146 or TR146/MUC1 samples, extracting the raw integrated density values of the green channel. Results were expressed in arbitrary units (AU). The difference between TR146 and TR146/MUC1 cells was tested by ANOVA.

2.8. Semi-quantification of MUC5B in cellular extracts by Dot-Blot

Dot Blot was performed on lysates of TR146 and TR146/MUC1 cells with a salivary pellicle. Three biological replicates were produced and analysed. Cells were lysed in 150 μl of RIPA buffer (Sigma–Aldrich) and proteins were quantified using the DC protein assay (Bio-Rad). The volume of lysate containing 5 μg of proteins was deposited per well on nitrocellulose membranes, in triplicate for each biological replicate. For detection of MUC5B, the primary antibody F2 (1:400 in PBS, 1 h) and the secondary antibody goat-anti mouse IgG coupled to HRP (LifeTechnologies, 1:2000, 1 h) were used. Non-specific binding was prevented using 0.3% fat-free milk. HRP activation was performed using the Clarity Western ECL Substrate Kit (Bio-Rad). Blot images were acquired using the Chemidoc imaging system (Bio-Rad). Semi-quantification of chemiluminescence detected within boundaries of each dot was performed using the ImageLab software. Results were expressed in arbitrary units (AU). The median values of technical replicates were calculated for each biological replicate, and the difference between TR146 and TR146/MUC1 cells was tested by ANOVA.

2.9. Scanning electron microscopy

Fixation of TR146 cells and TR146/MUC1 cells was carried out with 2.5% glutaraldehyde in PBS for 30 min, followed by 0.4% osmium tetroxide in PBS for 30 min. Dehydration was done through graded baths of ethanol (from 30 to 100%). Drying was performed by the critical point drying (CPD) method using Leica CPD 030. Samples were then coated with a thin carbon layer using a CRESSINGTON 308R and observed with a scanning electron microscope JEOL JSM 7600F (JEOL, Ltd.). SEM was operated at 2 kV and samples were observed at a working distance of 5 mm.

2.10. Immuno-scanning electron microscopy

Fixation of cells was achieved with 4% (v/v) paraformaldehyde for 20 min at 4 °C. Blocking and incubation with the antibody anti-MUC5B were performed as described for fluorescence immunostaining. The primary antibody was detected with 15 nm gold-labeled Goat Anti Mouse (GAM) IgG (Aurion, 1:15 in PBS, 1 h). After immunological reactions, samples were fixed with 2.5% glutaraldehyde in PBS. Finally, samples were dehydrated with ethanol, dried with CPD and carbon coated as described above. Samples were observed with a Hitachi SU5000 Schottky Field Emission—scanning electron microscope and gold particles were detected with a Backscattered Electron (BSE) detector. SEM was operated at 5 kV and samples were observed at a working distance of 8 mm.

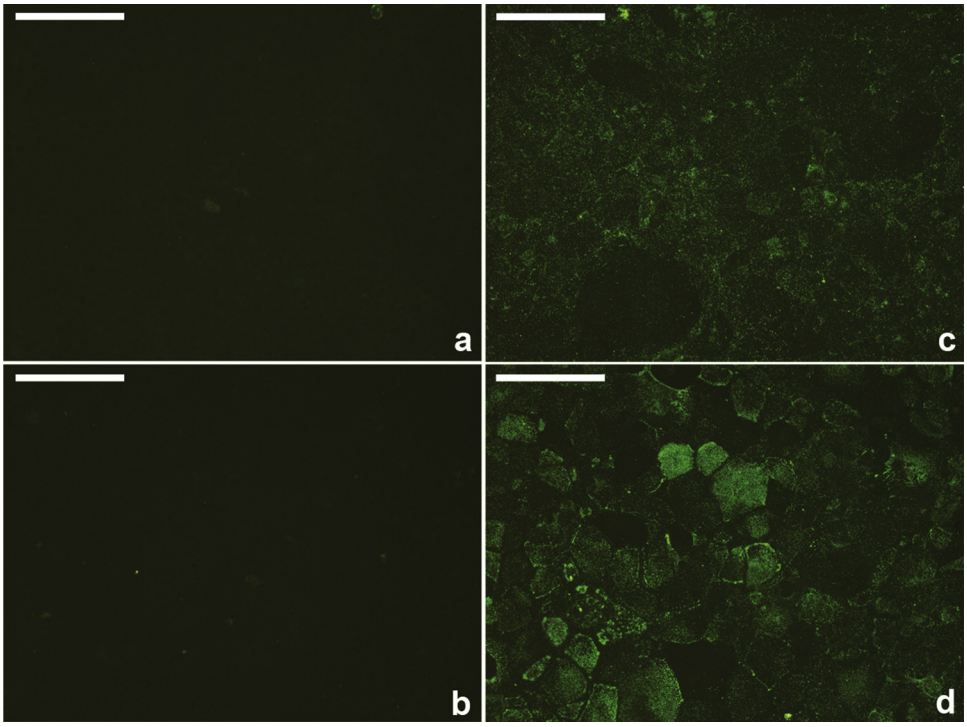

Fig. 3. MUC5B immunostaining of (a) TR146 cells, (b) TR146/MUC1cells, (c) TR146 cells incubated for 2 h with human saliva, (d) TR146/MUC1 cells incubated for 2 h with human saliva. Scale bars 100 μm.

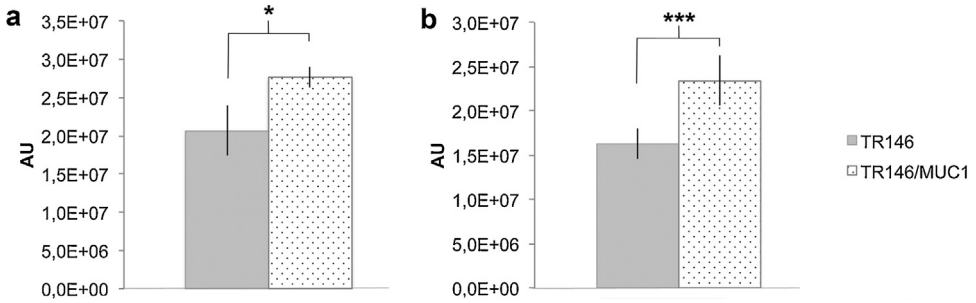

Fig. 4. Semi-quantification (mean ± STD) of MUC5B retained on TR146 and TR146/MUC1 cells after incubation for 2 h with human saliva by Dot-Blot chemiluminescence assay (a) and immunocytochemistry followed by image analysis (b).

3. Results

3.1. Expression of MUC1 in transfected cells

In order to confirm the efficiency of MUC1 transfection, RT-PCR and fluorescence immunostaining of MUC1 were carried on native TR146 cells and transfected TR146/MUC1 cells (Fig. 1). After amplification, the sequences AB and AC measuring 436 and 795 pb respectively were detected only in transfected cells (Fig. 1a), indicating that MUC1 was not detectable at the mRNA level in native cells and that transcription of the recombinant MUC1 gene was efficiently performed in the transfected cells. Compared to TR146 native cells (Fig. 1b), transfected TR146/MUC1 cells showed Alexa fluorescent green staining (Fig. 1c) that confirmed expression of MUC1 membrane-associated mucin at the protein level. Only some cells were stained, probably because superficial cells are not necessarily at the same stage of growth, inducing differences in MUC1 expression or MUC1 integration into the membrane.

3.2. Morphology of TR146 and TR146/MUC1 cells

After five days of growth, *i.e.*, three days after confluence was reached, cells formed a multi-layer culture whose thickness was approximated to 12.7 μm. No dead cells were observed (data not shown).

The cells surface was investigated by SEM and observations are presented in Fig. 2. The cells surface exhibited numerous membrane folds (microplicae) (Fig. 2a and c). These microplicae were clearly visualized at higher magnification (see arrows in Fig. 2b and d). The density and size of microplicae showed some cell-to-cell variability within one culture. However, overall, there was no substantial morphological difference between the two cell types.

3.3. Binding of saliva and MUC5B to TR146 and TR146/MUC1 cells

First, cell viability assays revealed that diluted clarified saliva was not toxic to cells for up to 24 h of exposure. Then, the ability of salivary mucins MUC5B to adsorb onto cells was evaluated by Dot-Blot which was performed on cells lysates, and by fluorescent immunostaining of cells. Fig. 3 shows immunostaining of MUC5B on cells and revealed that, expectedly, no fluorescence was detected in the absence of saliva (Fig. 3a and b). In contrast, MUC5B was detectable after incubation of cells with saliva for 2 h (Fig. 3c and d) on both cell types but not after incubation for 10 min (data not shown). TR146/MUC1 presented a higher fluorescent intensity than TR146, translating a higher amount of salivary MUC5B retained on the cells surface (Fig. 3c and d). Similarly to what was observed for MUC1 staining, clear between-cells variability was observed in the TR146/MUC1 culture while the lining appeared more homogenous in TR146 cells. From a semi-quantitative point of view (Fig. 4), TR146/MUC1 cells showed a significantly higher retention of salivary MUC5B than native TR146 cells indicated both by the Dot-Blot method (+34.1%, $p < 0.05$) and by immunocytochemistry (+44%, $p < 0.001$).

SEM allowed to observe the structure of the salivary deposit (Fig. 5a and b) and revealed that it was made of a loose filamentous network. No major differences were observed between transfected and native cells. Membrane folds were still visible under this network indicating that the saliva deposit was overall thin. However, some thicker and larger aggregates were also observed translating an uneven structure. SEM coupled to immunostaining of MUC5B was carried out (Fig. 5c) and it confirmed that the deposits contained MUC5B. The mesh size was approximated to a maximum of 0.5 μm.

4. Discussion

The objective of the present study was to evaluate the role of MUC1 in the anchoring of MUC5B onto oral epithelial cells, and more generally to obtain a deeper understanding of its involvement in the formation of the mucosal pellicle. Overall, we found that MUC5B binding was quantitatively enhanced when oral epithelial cells expressed MUC1. An in vitro model constituted of

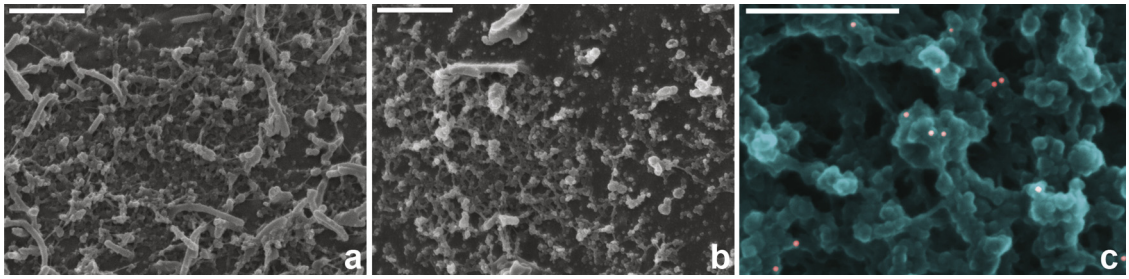

Fig. 5. SEM observations of TR146 (a) and TR146/MUC1 (b) cells, both incubated for 2 h with human saliva (scale bars 1 μm), and immuno-SEM detection of salivary MUC5B on salivary aggregates (scale bars 500 nm). Gold particles are coloured in pink. (For interpretation of the references to color in this figure legend, the reader is referred to the web version of this article.)

epithelial cells lined with a mucosal pellicle is proposed, based on the use of transfected TR146/MUC1 cells.

The experimental choice of using the TR146 cell line was guided by considerations on the structure of membrane-bound mucins and on the morphology of oral cells. Some epithelial cell lines are able to secrete membrane-bound mucins. For example, Gibbins et al. (2015) recently used HT29-MTX intestinal cells, which produce the membrane-bound mucins MUC5AC, to study mucosal pellicle formation. However, MUC5AC mucins can form a layer gel whose thickness varies from approximately 100–300 μm along the gastro-intestinal tract (Pelaseyed et al., 2014), which differs from the situation in the oral cavity where the pellicle thickness has been evaluated to a maximum of 100 nm (Morzel et al., 2014). Moreover, MUC5AC mucins do not possess the MUC1 amino-acid sequence which is thought to interact with MUC5B (Wang et al., 2004). Other human epithelial cell lines naturally express MUC1. MUC1 mRNAs were for example detected in several intestinal cell lines such as Caco-2 (Van Klinken et al., 1996). However, the morphology of intestinal cells differs quite substantially from that of oral cells, for example regarding their shape (columnar *vs* squamous) and the presence of microvilli at the apical surface of intestinal cells. In order to model closely the in vivo surface of oral mucosae, in particular that of soft tissues which represent the largest area in the oral cavity, we therefore opted for a well-characterized non-keratinized cell line, the TR146 cell line. TR146 also exhibits high similarity in terms of permeability with human oral cells (Jacobsen et al., 1995; Teubl et al., 2013). However, experiments performed in the present study indicated that MUC1 were not detectable in TR146 cells at the mRNA or protein level. Therefore, in order to study the involvement of MUC1 in oral mucosal pellicle formation, we stably transfected the TR146 cell line.

In the oral cavity, the thickness of the mucosa can vary from 500 and 800 μm (Wertz & Squier, 1991) with epithelial thickness varying from approximately 100 μm on the floor of the mouth to 300 μm on buccal surfaces (Prestin, Rothschild, Betz, & Kraft, 2012). The present model is thinner than oral epithelium and we suggest that it could represent the upper layer of mucosa, which directly interacts with compounds diluted in saliva. From a morphological point of view, non-keratinized surfaces of cheeks, lips or soft palate are made of cells characterised by membrane folds termed microplicae (Asikainen, Mikkonen, Ruotsalainen, Koistinen, & Kullaa, 2014, Kullaa-Mikkonen, 1986). Such folds were clearly present either on TR146 or on TR146/MUC1 cell membranes. This is particularly interesting knowing that these structures have been described as the basis for mucosal pellicle formation *in vivo*(Asikainen et al., 2012). Overall, SEM observations demonstrate that the morphologies of both types of cells are suitable for a model including a mucosal pellicle layer.

The ability of mucins MUC5B to bind to cells surface was demonstrated in both types of cells, and we showed that adsorption of salivary components to the mucosa is not immediate as indicated by undetectable MUC5B on cells incubated with saliva for 10 min. Furthermore, we noticed that with a longer incubation (24 h of incubation, data not shown), mucins formed dense and patchy aggregates, possibly due to local acidification by the cells. On synthetic surfaces also, time appears to be a determinant factor for mucin retention: MUC5B was detected on silica after 1 h incubation with saliva (Aroonsang et al., 2014) but was not after 20 min (Gibbins, Yakubov et al., 2014). The time used in the present study (2 h) was chosen to be compatible with the in vivo situation since the time of turnover of the superficial layer of oral epithelium was calculated to be 2.7 h (Dawes, 2003).

The specific mechanism of adsorption of MUC5B to oral surfaces is not fully elucidated to date. Some studies have demonstrated that MUC5B are retained better on hydrophobic than hydrophilic surfaces (Aroonsang et al., 2014; Cardenas et al., 2007) suggesting a role of hydrophobic effects. Moreover, the involvement of the membrane bound mucins MUC1 has also been proposed (Gibbins, Yakubov et al., 2014; Offner & Troxler, 2000). For example, Gibbins, Yakubov et al., 2014 and Gibbins, Proctor et al., 2014 pointed out that retention of MUC5B was limited on hydrophobic surfaces, and suggested that MUC1 is essential to pellicle formation. With regards to the possible biochemical interaction between the two mucins, an in vitro assay showed that multiple MUC5B domains could bind to the N-terminal domain of MUC1, especially with the last 107 amino acids (Wang et al., 2004). Here, our results provide an argument in favour of MUC1 implication, since TR146/MUC1 cells retained better MUC5B. Furthermore, the observation of between-cell variability in binding of salivary MUC5B to TR146/MUC1 cells may be correlated to the expression of MUC1 that was also observed to be uneven among the cells. However, bioadhesion of salivary mucins to epithelial cells, even if reduced, also occurred in TR146 cells. Thus the binding of MUC5B to epithelial cells is probably a multimodal process enhanced by the presence of membrane-associated mucins MUC1.

From a structural point of view, the salivary deposits observed by SEM both on TR146 and TR146/MUC1 cells were somehow comparable to the observations of human dried saliva (Teubl et al., 2013) where mucins form a filamentous network. However, the spatial organisation of mucins was different. In particular, the apparent mesh size is smaller in our model (up to 0.5 μm) than in dried saliva (up to 0.9 μm), which may be due to specific interactions of MUC5B with the underlying cell surface. The distribution of MUC5B over the surface of individual cells was comparable to the in vivo situation, where MUC5B appeared clustered on sections of buccal cells sampled on healthy subjects (Morzel et al., 2014). This clustering was all the more visible on TR146/MUC1 cells. In addition, although we did not observe by SEM structural differences of mucins network between TR146 and TR146/MUC1, the higher amount of MUC5B on TR146/MUC1 may have an impact on the pellicle functionality such as its lubricating properties. For example, Pramanik et al. (2010) related the reduction of oral lubrication in dry mouth patients with a lower expression of MUC1. Altogether, the model developed using TR146/MUC1 appeared to mimic more faithfully a healthy physiological situation compared to a TR146-based model.

As any in vitro model, the model presented in this study shows some limitations. First, no dead cells were observed and the nuclei integrity was preserved, which differs from the cell status in the superficial layer of a squamous non-keratinized epithelium previously described (Squier, 1991). Second, the MUC1/Y isoform of MUC1 expressed by TR146/MUC1 is a shorter form of the full-length human membrane-bound mucin that lacks the variable number tandem repeat (VNTR) region (Hanisch & Muller, 2000). Although the function of this region is not clearly described in epithelial oral cells, a correlation between its length and lubrication has been reported in eye epithelium (Imbert et al., 2006). The expression of MUC1 as a single isoform may therefore be a limitation to this model. Nevertheless, the model also presents several advantages. First, compared to synthetic surfaces, a cell-based model ensures that surface properties (*e.g.*, hydrophobicity, wettability, topography) are close to those found on oral mucosa and that salivary proteins can adopt a realistic spatial conformation. Second, it allows studying the biochemical interactions between cell membrane constituents and exogenous molecules, which would not be possible with a synthetic surface. Considering now cell-based models, to our knowledge, only one model based on oral cell cultures had previously taken into account the presence of a mucus layer lining the cells (Teubl et al., 2013). In that model, the mucus layer was dried prior to being deposited onto cells, which may affect its physico-chemical properties. In addition,

the mucus layer measured between 120 and 150 μm, *i.e.*, much thicker than the mucosal pellicle. In contrast, the present model is suitable to focus on the function and properties of the mucosal pellicle, especially since our model takes into consideration the expression of the membrane-bound MUC1, which enhanced the anchoring of MUC5B.

To conclude, the main advantage of the present model is to include a mucosal pellicle, *i.e.*, the layer at the interface between the oral epithelium and saliva. Its physico-chemical properties can control different mechanisms such as adsorption onto or diffusion through the mucosa. Therefore, this model is a promising tool to investigate molecular phenomena occurring at the surface of oral mucosae. As a perspective of this work, this model will be used to study the complex molecular interactions between flavour compounds, epithelial cells and the mucosal pellicle.

Acnowledgements

Prof Veerman (Free university of Amsterdam) is gratefully acknowledged for providing the MUC5B F2 antibody. The authors thank Christine Arnould (INRA, UMR1347 Agroécologie, ERL CNRS 6300, Plateforme DImaCell, Centre de Microscopie INRA/Université de Bourgogne) for confocal microscopy observations and Frédéric Herbst (Institut Carnot de Bourgogne, Université de Bourgogne) for training and assistance in SEM experiments. Hitachi High-Technologies Europe (Roland Schmidt) and Elexience (Thierry Grenut) are acknowledged for obtaining SEM images. Franck Ménétrier and Claire Fenech (Centre des Sciences du GoÛt et de l'Alimentation) are thanked for advice on sample preparation prior to microscopy and on RT-PCR, respectively. This study was funded by the French National Research Agency (Grant ANR-10-ALIA-001 MUFFIN). The French Ministry of Higher Education and Research provided the PhD fellowship for Sarah Ployon.

References

Aroonsang, W., Sotres, J., El-Schich, Z., Arnebrant, T., & Lindh, L. (2014). Influence of substratum hydrophobicity on salivary pellicles: organization or composition? *Biofouling*, *30*(9), 1123–1132.

Asikainen, P., Mikkonen, J. J., Ruotsalainen, T. J., Koistinen, A. P., & Kullaa, A. M. (2014). Microstructure of the superficial epithelial cells of the human oral mucosa. *Ultrastructural Pathology*, *38*(1), 6–12.

Asikainen, P., Ruotsalainen, T. J., Mikkonen, J. J. W., Koistinen, A., ten Bruggenkate, C., & Kullaa, A. M. (2012). The defence architecture of the superficial cells of the oral mucosa. *Medical Hypotheses*, *78*(6), 790–792.

Boegh, M., & Nielsen, H. M. (2015). Mucus as a barrier to drug delivery – understanding and mimicking the barrier properties. *Basic & Clinical Pharmacology & Toxicology*, *116*(3), 179–186.

Bradway, S. D., Bergey, E. J., Jones, P. C., & Levine, M. J. (1989). Oral mucosal pellicle: adsorption and transpeptidation of salivary components to buccal epithelial cells. *Biochemical Journal*, *261*(3), 887–896.

Bradway, S. D., Bergey, E. J., Scannapieco, F. A., Ramasubbu, N., Zawacki, S., & Levine, M. J. (1992). Formation of salivary mucosal pellicle: the role of transglutaminase. *Biochemical Journal*, *284*, 557–564.

Cardenas, M., Elofsson, U., & Lindh, L. (2007). Salivary mucin MUC5B could be an important component of in vitro pellicles of human saliva: an in situ ellipsometry and atomic force microscopy study. *Biomacromolecules*, *8*(4), 1149–1156.

Chang, W.-I., Chang, J.-Y., Kim, Y.-Y., Lee, G., & Kho, H.-S. (2011). MUC1 expression in the oral mucosal epithelial cells of the elderly. *Archives of Oral Biology*, *56*(9), 885–890.

Dawes, C. (2003). Estimates, from salivary analyses, of the turnover time of the oral mucosal epithelium in humans and the number of bacteria in an edentulous mouth. *Archives of Oral Biology*, *48*(5), 329–336.

Gibbins, H. L., Proctor, G. B., Yakubov, G. E., Wilson, S., & Carpenter, G. H. (2014). Concentration of salivary protective proteins within the bound oral mucosal pellicle. *Oral Diseases*, *20*(7), 707–713.

Gibbins, H. L., Proctor, G. B., Yakubov, G. E., Wilson, S., & Carpenter, G. H. (2015). SIgA binding to mucosal surfaces is mediated by mucin–mucin interactions. *PLoS One*, *10*(3), 13. http://dx.doi.org/10.1371/journal.pone.0119677.

Gibbins, H. L., Yakubov, G. E., Proctor, G. B., Wilson, S., & Carpenter, G. H. (2014). What interactions drive the salivary mucosal pellicle formation? *Colloids and Surfaces B-Biointerfaces*, *120*, 184–192.

Hanisch, F. G., & Muller, S. (2000). MUC1: the polymorphic appearance of a human mucin. *Glycobiology*, *10*(5), 439–449.

Hannig, M., & Joiner, A. (2006). The structure, function and properties of the acquired pellicle. *Monographs in Oral Science*, *19*, 29–64.

Hay, D. I. (1967). The adsorption of salivary proteins by hydroxyapatite and enamel. *Archives of Oral Biology*, *12*(8), 937–946.

Imbert, Y., Darling, D. S., Jumblatt, M. M., Foulks, G. N., Couzin, E. G., Steele, P. S., et al. (2006). MUC1 splice variants in human ocular surface tissues: possible differences between dry eye patients and normal controls. *Experimental Eye Research*, *83*(3), 493–501.

Jacobsen, J., Van Deurs, B., Pedersen, M., & Rassing, M. R. (1995). TR146 cells grown on filters as a model for human buccal epithelium: I. Morphology, growth, barrier properties, and permeability. *International Journal of Pharmaceutics*, *125*(2), 165–184.

Kullaa, A. M., Asikainen, P., Herrala, M., Ukkonen, H., & Mikkonen, J. J. W. (2014). Microstructure of Oral Epithelial Cells as an Underlying Basis for Salivary Mucosal Pellicle. *Ultrastructural Pathology*, *38*(6), 382–386.

Kullaa-Mikkonen, A. (1986). Scanning electron microscopic study of surface of human oral mucosa. *European Journal of Oral Sciences*, *94*(1), 50–56.

Morzel, M., Tai, S., Brignot, H., & Lherminier, J. (2014). Immunocytological detection of salivary mucins (MUC5B) on the mucosal pellicle lining human epithelial buccal cells. *Microscopy Research and Technique*, *77*(6), 453–457.

Nayak, A., & Carpenter, G. H. (2008). A physiological model of tea-induced astringency. *Physiology & Behavior*, *95*(3), 290–294.

Offner, G. D., & Troxler, R. F. (2000). Heterogeneity of high-molecular-weight human salivary mucins. *Advances in Dental Research*, *14*, 69–75.

Pelaseyed, T., Bergstrom, J. H., Gustafsson, J. K., Ermund, A., Birchenough, G. M. H., Schutte, A., et al. (2014). The mucus and mucins of the goblet cells and enterocytes provide the first defense line of the gastrointestinal tract and interact with the immune system. *Immunological Reviews*, *260*(1), 8–20.

Pramanik, R., Osailan, S. M., Challacombe, S. J., Urquhart, D., & Proctor, G. B. (2010). Protein and mucin retention on oral mucosal surfaces in dry mouth patients. *European Journal of Oral Sciences*, *118*(3), 245–253.

Prestin, S., Rothschild, S. I., Betz, C. S., & Kraft, M. (2012). Measurement of epithelial thickness within the oral cavity using optical coherence tomography. *Head and Neck-Journal for the Sciences and Specialties of the Head and Neck*, *34*(12), 1777–1781.

Rat, P., Korwinzmijowska, C., Warnet, J. M., & Adolphe, M. (1994). New in-vitro fluorimetric microtitration assays for toxicological screening of drugs. *Cell Biology and Toxicology*, *10*(5–6), 329–337.

Rupniak, H. T., Rowlatt, C., Lane, E. B., Steele, J. G., Trejdosiewicz, L. K., Laskiewicz, B., et al. (1985). Characteristics of 4 new human cell lines derived from squamous cell carcinomas of the head and neck. *Journal of the National Cancer Institute*, *75*(4), 621–635.

Sengupta, A., Valdramidou, D., Huntley, S., Hicks, S. J., Carrington, S. D., & Corfield, A. P. (2001). Distribution of MUC1 in the normal human oral cavity is localized to the ducts of minor salivary glands. *Archives of Oral Biology*, *46*(6), 529–538.

Squier, C. A. (1991). The permeability of oral mucosa. *Critical Reviews in Oral Biology and Medicine*, *2*(1), 13–32.

Tabak, L. A., Levine, M. J., Mandel, I. D., & Ellison, S. A. (1982). Role of salivary mucins in the protection of the oral cavity. *Journal of Oral Pathology & Medicine*, *11*(1), 1–17.

Teubl, B. J., Absenger, M., Froehlich, E., Leitinger, G., Zimmer, A., & Roblegg, E. (2013). The oral cavity as a biological barrier system: design of an advanced buccal in vitro permeability model. *European Journal of Pharmaceutics and Biopharmaceutics*, *84*(2), 386–393.

Van Klinken, B. J. W., Oussoren, E., Weenink, J. J., Strous, G. J., Buller, H. A., Dekker, J., & Einerhand, A. W. C. (1996). The human intestinal cell lines Caco-2 and LS174T as models to study cell-type specific mucin expression. *Glycoconjugate Journal*, *13*(5), 757–768.

Wang, L., Li, X., Bruno, L., Oppenheim, F. G., Troxler, R. F., & Offner, G. D. (2004). MUC1 and MUC5B can form a protective mucin scaffold. *Paper presented at the international association for dental research annual meeting*, Hawai Convention Center, Honolulu.

Wertz, P. W., & Squier, C. A. (1991). Cellular and molecular basis of barrier function in oral epithelium. *Critical Reviews in Therapeutic Drug Carrier Systems*, *8*(3), 237–269.